External magnet improves antitumor effect of vinblastine and the suppression of metastasis

Suman Dandamudi,[1] Vishwesh Patil,[1] William Fowle,[2] Ban-An Khaw[1] and Robert B. Campbell[1,3]

[1]Department of Pharmaceutical Sciences, Bouvé College of Health Sciences, and [2]Department of Biology, Arts and Sciences, Northeastern University, Boston, Massachusetts, USA

(Received February 16, 2009/Revised March 30, 2009/Accepted April 19, 2009/Online publication May 15, 2009)

The use of magnetic drug targeting (MDT) to selectively deliver chemotherapeutic drugs to tumor cells is a widely investigated approach; however, the notion of targeting tumor endothelial cells by this method is a fairly new concept. Positively-charged (cationic) liposomes have an extraordinarily high affinity for tumor vessels, but heterogeneous targeting is frequently observed. In order to improve on the overall efficiency of targeting tumor vessels, we investigated the use of an externally applied magnetic field together with magnetic cationic liposomes (MCLs) for cancer treatment. We examined the antitumor effect of the chemotherapeutic agent vinblastine loaded in MCLs, using a murine model of melanoma. Two hours following i.v. administration of MCLs, we observed significant tumor vascular uptake with use of an external magnet (15.9 ± 6.3%) compared to no magnet (5 ± 1.3%). The administration of vinblastine-loaded MCLs with the magnet produced a significant antitumor effect, reducing the presence of tumor nodules in preferential sites of metastasis compared to untreated and free drug control groups. CD31 immunostaining revealed a decrease in the general length of tumor blood vessels, altered vascular morphology and interruptions in the tumor vascular lining for the vinblastine-loaded MCL groups. Drug-loaded MCLs with magnetic fields may represent a promising combination approach for cancer treatment. (*Cancer Sci* 2009; 100: 1537–1543)

The growth and survival potential of a tumor depends on its ability to successfully recruit neovascular networks.[1] Any injury caused to the developing (or mature) vascular supply will impair general tumor function(s), limiting the flow of oxygen and nutrients to cancer cells.[2,3] Vascular targeting is thus a rational therapeutic approach, and the use of cationic (positively-charged) liposomes has been shown to improve the overall efficiency of targeting.[4–6]

Chemotherapy is considered a popular choice for the treatment of local and disseminated disease; the treatment outcome varies according to tumor type, stage, and strategy. Unfortunately, owing to the relatively non-specific action of conventional agents, severe side effects are a major concern. Magnetic drug targeting (MDT) has been used to improve the selective delivery of chemotherapeutic agents to tumors, reducing their uptake by healthy tissues and drug-associated side effects.[7–15] In MDT, an external magnetic field is applied to increase the concentration of the drug at the target site. The combination of improved target selectivity and increased exposure time of drug to the tumor should also diminish the amount of drug recovered by the reticuloendothelial system.[8]

Magnetic drug targeting (MDT) was first introduced by Widder *et al.* for site-specific delivery of adriamycin-loaded magnetic albumin microspheres.[7] Magnetic liposomes have been reported for use in a wide range of biomedical and diagnostic applications such as cell growth, MRI, hyperthermia, and localized drug targeting.[11,16,17] The approach has been developed to deliver DNA, RNA, and other therapeutic molecules to target tissues.[9,10,14,18–20]

In the present study, the chemotherapeutic agent vinblastine sulfate was loaded in Pegylated cationic liposomes (PCLs). Magnetite was also loaded to produce magnetic cationic liposomes (MCLs); when magnetic fields are applied, MCLs are significantly more responsive to the strength of the magnetic field compared to PCLs. MCLs were previously characterized in terms of their general susceptibility to magnetic fields and other physicochemical properties, including size, membrane fluidity, surface charge, and drug-loading potential.[21,22] The rationale for combining cation-mediated tumor targeting with MDT was partially based on the observation that the loading of magnetite (MAG-C) in cationic liposomes did not prevent vascular targeting from occurring (at the concentration and ratio of magnetite to PCLs used).[21] The inclusion of PEG in MCLs significantly reduced the uptake of MCLs by the liver, lung, and spleen while preserving their vascular targeting characteristics.[21,22] The goal of the present study was now to quantify the percent of tumor vascular areas targeted with MCLs both in the absence and presence of an externally applied magnetic field, and to determine the overall significance of the treatment approach using vinblastine-loaded MCLs in a murine model of melanoma.

Materials and Methods

Preparation of magnetic liposomes. Liposomes were prepared by thin lipid film and hydration method.[21] Briefly, DMPC, DMTAP, CHOL, and DMPE-PEG_{5000} (35:50:10:5) purchased from Avanti Polar Lipids (Alabaster, AL, USA) were mixed in specific ratios and a thin film was formed using a rotary evaporator. The freeze-dried film was hydrated with MAG-C solution (aqueous dispersion of magnetite, iron content 72%) from Chemicell (Berlin, Germany). Liposomes were then sonicated and centrifuged at 1000 *g* for 15 min to remove unincorporated MAG-C.[10,21]

Preparation of vinblastine-loaded MCLs. Drug-loaded MCLs were prepared by mixing the required amount of lipids and vinblastine sulfate purchased from Sigma Chemicals (St. Louis, MO, USA) in a round bottom flask to obtain 5 mole% (drug to lipid ratio) of drug. The total lipid concentration was 20 μmol/mL and MAG-C was 5 mg/mL. The unincorporated drug was separated from drug-loaded MCLs by dialysis and the percent of vinblastine loaded was determined by HPLC.[22,23]

Transmission electron microscopy (TEM) studies. HMEC-1 cells were seeded on a sterile 199-μm thick ACLAR film in a six-well plate at a density 5×10^5 cells/mL. The cells were allowed to adhere on the ACLAR film for 24 h in the required growth medium. Cells were incubated for 24 h at 37°C in a humidified atmosphere of 5% CO_2. Cells were either exposed to (2.5 mg/mL of) MAG-C or cationic liposomes (250 nmoles) for 24 h following the initial incubation period. Twenty-four h later the required growth media was removed and cells were washed with PBS to separate unbound liposomes from the cellular-bound fraction. To view the cellular localization of magnetic liposomes, cells were initially

[3]To whom correspondence should be addressed. E-mail: r.campbell@neu.edu

doi: 10.1111/j.1349-7006.2009.01201.x

fixed with 2.5% glutaraldehyde and 2.0% formaldehyde in 0.1-M sodium cacodylate buffer (pH 7.2) for 30 min at 4°C. The cells were then rinsed with 0.1-M sodium cacodylate buffer (pH 7.2) for 20 min with two changes. The cells were then post-fixed with 1% osmium tetroxide in 0.1-M sodium cacodylate buffer (pH 7.2) for 1 h at room temperature. Cells were washed with 0.1-M sodium cacodylate buffer (pH 7.2) for 20 min with two changes to remove excess osmium tetroxide. The cells were then dehydrated with series of graded ethanol to 100% and transferred to n-butyl glycidyl ether for 45 min with two changes. These ACLAR films were then placed in Queto-spurr resin[24] and polymerized at 60°C for 24 h. At the end of 24 h, the cells were embedded into the resin and the film was stripped off the resin. A piece of resin was then cut and glued on epoxy resin capsules using 5 Minute Epoxy (Fisher Scientific, Suwanee, GA, USA). Thin sections were then made using ultracut microtone (Leica Microsystems, Bannock, IL) and collected on copper grid (mesh size, 200). The sample with cells only was stained with 5% uranyl acetate and Reynolds lead citrate, whereas samples of cells treated with MAG-C or cationic liposomes containing MAG-C were unstained. Finally, samples were viewed under TEM.

Tumor cell implantation and other studies *in vivo*. For the experiments involving the use of mice, our animal protocol was first approved by the Institutional Animal Care and Use Committee at Northeastern University (NEU), Boston, MA, USA. All of the animal work was performed in accordance with the institutional guidelines in approved NEU facilities.

Gamma imaging. B16-F10 melanoma cells were injected subcutaneously into SCID mice and were allowed to grow until tumors reached 250 mm^3 in size. To these mice, ^{111}In labeled MAG-C cationic liposomes (containing 2.5 mg/mL) were injected intravenously, and some mice were exposed to the external magnet (neodymium, 1.2 T) purchased from Master Magnetics (Castle Rock, CO, USA) for 1 h. Images were acquired 2 h following tail vein injection using a single-photon emission computed tomography (SPECT) imager equipped with pin-hole collimator (Jefferson's Lab, Newport News, VA, USA). Twenty-min images were obtained in a 23.5×12.46 cm field of view with a photo peak window set at 514 Kev. Images were then processed by K-MAX imaging software and corrected using flood images as the background.

Intravital microscopy. Male SCID mice (10–12 weeks old) were anesthetized using a mixture of ketamine and xylazine. Dorsal skinfold chambers were made as described elsewhere.[5] Melanoma cells (2×10^6) were injected subcutaneously into SCID mice and tumors were allowed to grow until they reached the size of 200 mm^3. Tumors were then surgically removed under asceptic conditions, minced into small pieces, and a single piece was placed in the center of the dorsal skinfold chamber window. When approximately half the total window area of the dorsal chamber was occupied by the tumor, an amount of 0.1 mL of rhodamine-labeled MAG-C cationic liposomes (20 μmol/mL) was injected intravenously into tail vein of the mouse. To generate a magnetic field within the window, a small round-shaped external magnet (1.2 T, 0.5 inch × 0.5 inch) was placed on the opposite side of the window for 1 h. Two hours post injection, 0.1 cc of 2-million MW FITC-dextran (15 mg/mL) was injected via the tail vein to view the functional blood supply. Fluorescence microscopy was used to determine the location of the liposomes with respect to the tumor vasculature. Images were acquired first in the FITC channel (to view blood vessels) and then in the rhodamine channel (to view the liposomes). The two images were then blended to observe liposomes distributed along tumor vessels. The blended images were then quantified using Bioquant Imaging Software (Bioquant Imaging Analysis Corporation, Nashville, TN, USA). Regions were randomly selected in the tumor and pixel counts of green and red fluorescence were calculated. Percent of tumor vascular accumulation was calculated as follows:

$$= \frac{\text{Total pixel counts of liposomes (red channel)}}{\text{Total pixel counts of blood vessels (green channel)}} \times 100$$

Treatment groups and chemotherapy. Melanoma tumors were developed in female SCID mice (20 gm) by injection of 0.1 cc (1×10^6 cells) of B16-F10 cells subcutaneously. Mice were divided into four treatment groups containing five to six mice in each group. On day 12, or when tumor volume reached 100 mm^3, different preparations of vinblastine sulfate were administered via tail vein injection. Group 1 was the control, and these mice received saline. Group 2 received free vinblastine sulfate at a dose of 1.35 mg/kg. Group 3 received vinblastine loaded in MCLs at a dose equivalent to group 2 (lipid- 20 μmol/mL, MAG-C-5 mg/mL) without external magnet; and for group 4, external magnet (1.2 T) was placed on the external tumor surface for 1 h.

Mice were monitored daily through out the study and changes in tumor volume were measured using digital calipers (Control Company, Friendswood, TX, USA). The tumor volume (mm^3) was calculated using the following formula:

$$V = 0.52(\text{Length})(\text{width})^2$$

Percent change in tumor volume was calculated as follows:

$$\frac{\text{Tumor volume on day 16} - \text{Tumor volume on 1st day of injection}}{\text{Tumor volume on 1st day of injection}} \times 100$$

Immunohistochemistry. Mice were sacrificed; and the liver, spleen, lung, and tumors were collected. The tissues were fixed with paraformaldehyde, embedded in paraffin and cut into thin sections. H&E staining was performed on these thin sections by standard procedure. To visualize blood vessels, CD31 staining was performed on the sections using conventional staining methods. Briefly, thin tumor sections were incubated with rat anti-mouse CD31 antibody (dilution, 1:3) (catalog no. 553370; BD-Pharmingen, Sandiego, CA, USA). A goat anti-rat antibody with horseradish peroxidase was used as the secondary antibody. Next, chromogen 3, 3′-diaminobenzidine tetrahydrochloride was added to the sections followed by counterstaining with hematoxylin, and sections were mounted on slides for analysis.

Statistical analysis. The-non-parametric Mann–Whitney *U*-test was used to determine statistically significant differences between two experimental groups and ANOVA was used to evaluate more than two groups. *P*-values ≤ 0.05 were considered statistically significant.

Results

Transmission electron microscopy (TEM) studies. To determine whether drug-loaded MCLs accumulate in tumor endothelial cells, we evaluated the uptake of MCLs by HMEC-1 cells, our cellular model of the tumor vasculature. Micrographs of untreated cells show cellular organelles including the nucleus and cytoplasm (Fig. 1a). The micrograph of cells exposed to MAG-C alone showed clear dark spots indicating the presence and uptake of MAG-C (Fig. 1b). In micrographs of HMEC-1 cells exposed to MCLs for 24 h, the dark spots were similar to those observed in the MAG-C alone group (Fig. 1c). Prior to exposing cells to liposomes, the unincorporated MAG-C was separated from MCLs, and hence, the dark particles correspond to the presence of MAG-C in the liposomes and not free MAG-C. MAG-C cationic liposomes were also observed in endosomes indicating the internalization of liposomes by endocytosis, with localization of MCLs around (but not in) the nucleus.

Gamma imaging. We evaluated the effect of the external magnet (1.2 T, 1 h) *in vivo* on tumor uptake of MCLs in melanoma-bearing SCID mice. Nobuto *et al.* have studied the application of magnetic fields on the accumulation of doxorubicin in tumors. The authors

doi: 10.1111/j.1349-7006.2009.01201.x

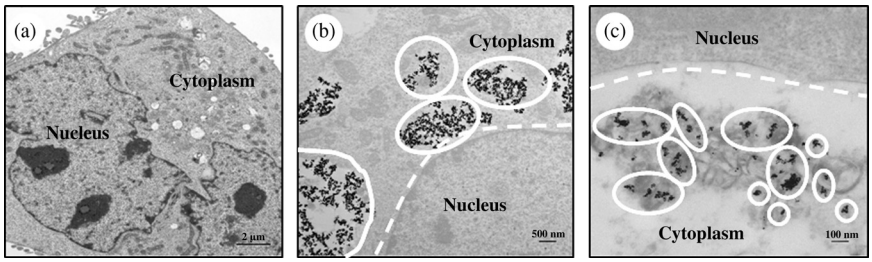

Fig. 1. Transmission electron microscopy (TEM) images of cells. Human dermal microvascular endothelial (HMEC)-1 cells were seeded in a six-well plate and either free fluid MAG-CS (magnetite, citric acid matrix) (MAG-C) or cationic liposomes containing MAG-C was added to cells. Images were acquired from TEM for cells alone (a), cells treated with MAG-C (b) or with cationic liposomes containing MAG-C (c). Circles in (b,c) indicate MAG-C.

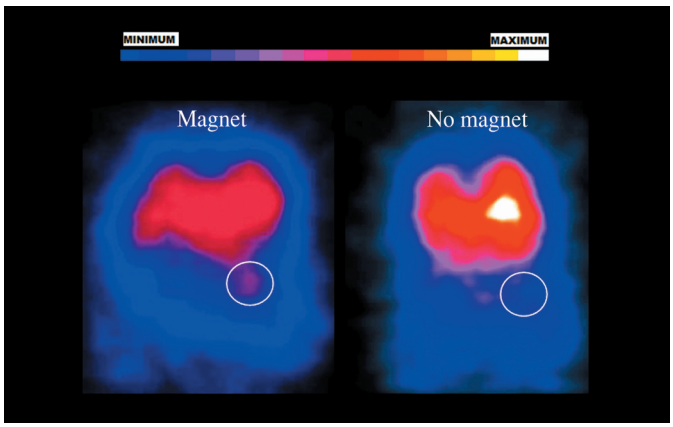

Fig. 2. *In vivo* anterioposterior gamma images of melanoma tumor in SCID mice. B16-F10 murine melanoma tumors were grown subcutaneously in mice and injected with ^{111}In labeled free fluid MAG-CS (magnetite, citric acid matrix) (MAG-C) cationic liposomes. A magnet (1.2 T) was placed on the external surface of tumor for 1 h. Approximately 2 h following injection, images of mice were acquired using a gamma camera. The circle represents the exact location of tumor.

showed that an increase in the application time of the electromagnetic field (up to 60 min) increased the concentration of doxorubicin within the tumor. However, no additional increase in tumor doxorubicin concentration was observed with 100-min application of magnetic field.[11] In the present study, the external magnet was placed for 1 h. We observed a greater signal in tumors previously exposed to the external magnet (exposure time, 1 h) compared to the no-magnet group (Fig. 2). The use of an external magnet thus improved the accumulation and retention of MCLs in the tumors.

Accumulation of MCLs in tumor vasculature. Melanomas grow well in mice-bearing dorsal skinfold chambers (DSC).[25–27] Pluen *et al.* have grown melanoma (Mu89) tumors in DSC to study diffusion of particles in the tumor interstitial matrix.[27] Krasnici *et al.* studied the influence of surface charge potential on the vascular distribution of liposomes in DSC using A-Mel-3 (a amelanotic hamster melanoma).[25] Herein, we studied vascular accumulation of MCLs in B16-F10 tumors in mice-bearing DSC.

Tumor vascular targeting using cationic liposomes can be achieved in the presence of magnetite (MAG-C),[4,5,22] since the relatively high incorporation of MAG-C did not prevent targeting.[22] In the present study, we determined whether a magnet applied to the external surface of the tumor could be used to alter the extent to which MCLs accumulate along the tumor vasculature. The percent vascular area covered with MAG-C cationic liposomes in the absence and presence of the magnet was 5 ± 1.3 and $16 \pm 6.3\%$, respectively (Fig. 3d). The magnet thus enhanced the

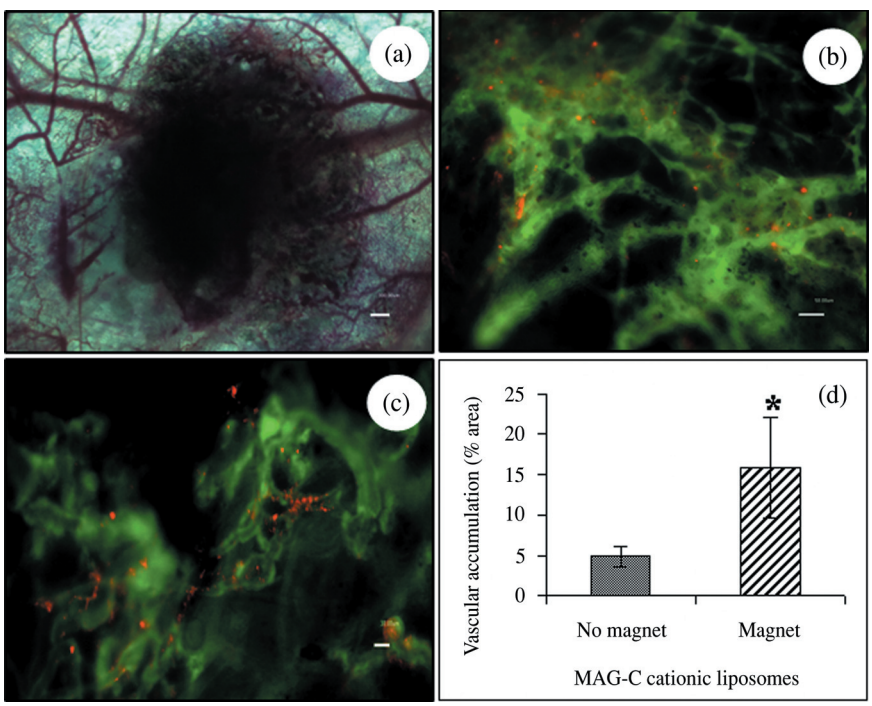

Fig. 3. Accumulation of magnetic cationic liposome (MCL) in tumor blood vessels. For intravital microscopic analysis, a melanoma (B16-F10) tumor piece was implanted in the center of dorsal skinfold chamber (a). An amount of 0.1 mL of rhodamine labeled MCLs (20 μmol/mL) was injected i.v. into the tail vein of the mouse and an external magnet (1.2 T) was placed on the opposite side of the window for 1 h. Two hours following injection, 0.2 cc of 2-million MW FITC-dextran (15 mg/mL) was injected via the tail vein to view the functional blood supply. Fluorescence microscopy images show tumor vascular accumulation of MCLs in the absence (b) and presence of the magnet (c). Each value represents mean ± SD, $P \leq 0.05$ (bar = 50 μm).

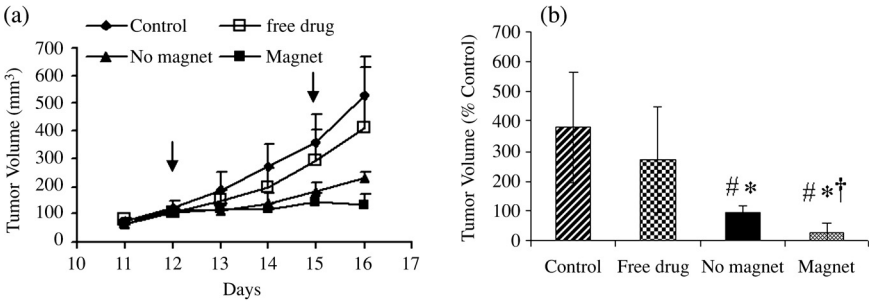

Fig. 4. Antitumor effects of intravenously administered vinblastine preparations on B16-F10 murine melanoma tumor growth. The control group received saline and the treatment groups received either free vinblastine (1.35 mg/kg) or drug loaded in magnetic cationic liposomes (MCLs) in the absence and presence of an externally applied magnet (1.2 T, 1 h). Each value represents the mean ± SD of six mice. #$P \leq 0.05$ compared to control, *$P \leq 0.05$ compared to free drug, †$P \leq 0.05$ compared to no magnet. Arrows indicate day of injections.

uptake of MCLs by the tumor vasculature, suggesting that the MDT approach might improve the delivery of therapeutic agents to this site as well.

Efficacy evaluation. Mice were randomly divided into four treatment groups (see "Materials and Methods"). All tumor volumes were monitored daily as shown in Figure 4. In the control group we observed rapid tumor growth, with tumor volumes reaching approximately 700 mm^3 within 5 days following the first injection. A thick and callous layer formed on some tumor surfaces forcing an untimely termination of the study for mice in this group. In mice treated with free vinblastine sulfate (1.35 mg/kg), we observed no significant difference in the tumor volumes when compared to the untreated control group. Heterogeneous tumor growth was observed in the untreated and free vinblastine control groups. There was less heterogeneity in terms of tumor sizes in the vinblastine-loaded MCLs group; the magnetic field enhanced the tumor response to the formulation when compared to free vinblastine and untreated control group. When the external magnet was applied, the tumor volumes remained relatively constant (no increase in overall volume when compared to day 1 of treatment).

On day 16 there was a significant difference in the antitumor effects of vinblastine-loaded MCLs in the presence of an external magnet compared to no magnet (Fig. 4a). The external magnet reduced the tumor volume (131 ± 37 mm^3) to a significantly greater extent compared to no magnet (227 ± 22 mm^3). At the end of the experiment, the percent of change in tumor volume was significantly lower for the formulation (24 ± 32%) in the presence of a magnet when compared to the no-magnet (94 ± 21%), free vinblastine (270 ± 177%), and untreated (378 ± 185%) groups (Fig. 4b).

Histological analysis. Following the completion of the tumor efficacy study, all mice were sacrificed and the liver, spleen, lung, and tumors were removed. The paraffin-embedded tissue sections were stained with H&E. Light microscopy images of H&E sections of tumors from different treatment groups are shown in Figure 5(a). The intense blue hematoxylin staining of tumor sections removed from the mice in the control group indicates viable cells in tissue. We observed no difference in tumor cell density between free vinblastine and saline control groups; this was consistent with the tumor volume measurements. We observed a decrease in the number of viable cells in the tumor sections from mice treated with the drug-loaded MCL formulations compared to the untreated and free drug control groups, and the external magnet further reduced the general population of stained nuclei when compared to no magnet (Fig. 5a).

Tumor metastases. Melanoma tumors originate from melanocytes and produce excessive melanin pigmentation.[28] The presence of melanin pigmentation in the different organs was used to track tumor metastasis, since under normal conditions melanin is not present in healthy SCID mice. The primary sites of melanoma metastases are lung, liver, lymph nodes, spleen, brain, and intestines.[29] The H&E images of liver and spleen showed no significant differences in nuclei staining between the different treatment groups. We found relatively high melanin pigmentation in the liver and spleen of the saline control group (Fig. 5a). This would suggest that the primary tumor metastasized to these organs.

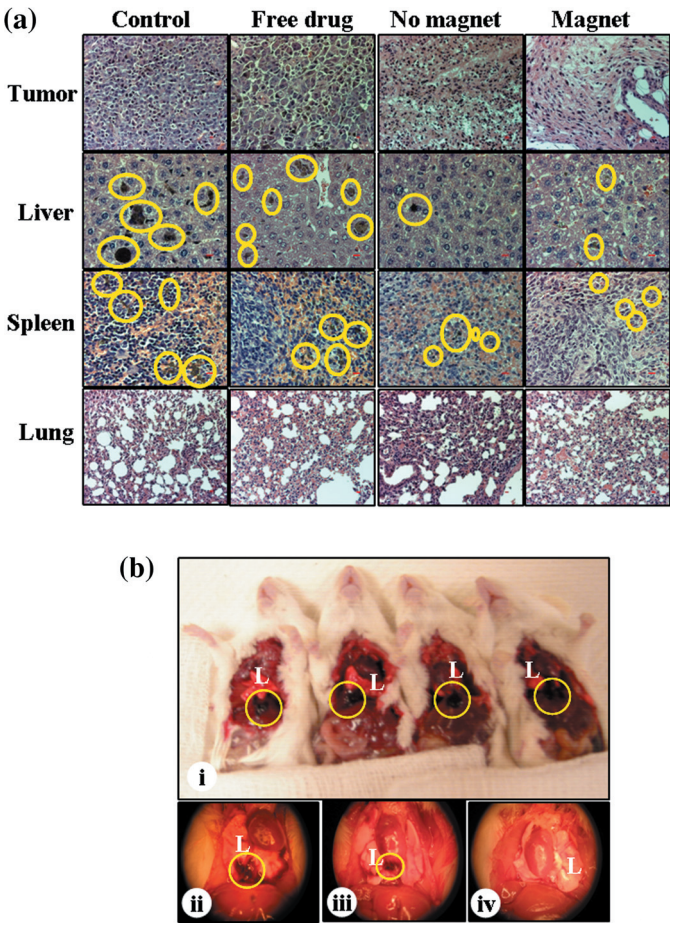

Fig. 5. Histopathology. Formalin-fixed, paraffin-embedded tissue sections of different organs such as the tumor, liver, spleen, and lung were stained with hematoxylin–eosin (a). Magnification 20× (bar = 10 μm). Pictures of tumor metastasis of pleural cavity (b). Control mice (b[i]), free vinblastine (b[ii]), vinblastine-loaded magnetic cationic liposomes (MCLs) without magnet (b[iii]) and with magnet (b[iv]). Pictures are representative of mice from each treatment group. The circle denotes melanin pigment, reveals invasiveness of melanoma tumor in liver, spleen, and pleural cavity.

The number of tumor nodules was less in the livers of mice treated with free vinblastine sulfate compared to the saline control. We also found melanin pigmentation in tissue sections of mice treated with vinblastine-loaded MCLs in the absence and presence of an external magnet, but relatively less compared to the other treatment groups.

All mice (5/5) in the saline- and free-vinblastine-treated groups showed evidence of metastasis within the pleural cavity (Fig. 5b[i, ii]). In the group treated with vinblastine-loaded MCLs having no exposure to the magnet, two out of five (40%) mice showed

doi: 10.1111/j.1349-7006.2009.01201.x

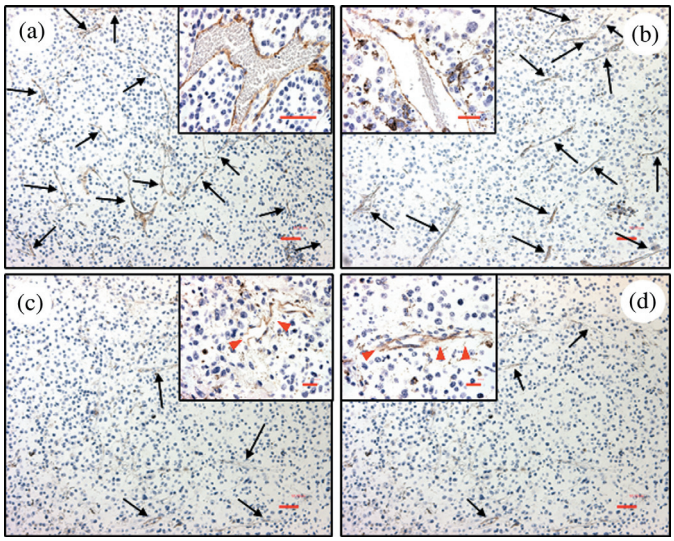

Fig. 6. CD31 staining of formalin-fixed tumor sections of different treatment groups. Control group (a), free vinblastine group (b), vinblastine-loaded magnetic cationic liposomes (MCLs) without (c) and with magnet (d). Images are representative of mice from each treatment group. Black arrows indicate CD31 (brown) staining and red arrows show discontinuous CD31 staining. Magnification 10× (bar = 50 μm). Inserted picture magnification 40× (bar = 50 μm).

no signs of metastasis, and the remaining three mice in group showed relatively less in comparison to the saline control and free vinblastine groups (Fig. 5b[iii]). On the other hand, we did not observe any signs of metastasis in the pleural cavity of mice in the magnet group (Fig. 5b[iv]). The external magnet probably retained a significantly higher fraction of the drug within the tumor, severely compromising the tumor's ability to metastasize to the pleural cavity. The s.c. injection of B16-F10 cells did result in the formation of detectable lung metastases within the first 16 days; however, regardless of the treatment group, no melanin pigmentation was observed in the lung parenchyma of any mouse in study. This is unlike studies involving the intravenous injection route, where the aggressive cellular phenotype rapidly forms tumor nodules within the lung parenchyma.

Immunohistochemistry. The application of an external magnet significantly improved the antitumor activity of vinblastine-loaded MCLs when compared to all other groups. We next asked whether the average number of tumor vessels following treatment was consistent with the overall treatment outcome. To this end, we sacrificed all mice at the end of the study, tumors were collected, and CD31 staining was performed to acquire vessel density measurements. The light microscopy images of CD31 staining of tumor tissue sections are shown in Figure 6. The vinblastine loaded in the MCLs group showed fewer blood vessels when compared to the saline control and free drug group. The number of blood vessels of the saline control group (64 vessels/mm^2) was similar to free vinblastine group (63 vessels/mm^2); control values are consistent with reports elsewhere for B16-F10 sections at 20× magnification.[30] The number of tumor blood vessels for the formulation groups in the absence (49 vessels/mm^2) and presence (52 vessels/mm^2) of the external magnet was relatively less by comparison.

Although the number of blood vessels observed in the magnet and no-magnet group was similar, we did observe some interesting qualitative therapeutic effects. We noted discontinuities in the lining of the vessel wall, and a general decrease in the length of tumor vessels and altered vascular morphology in mice treated with the formulation (Fig. 6c,d), compared to the other groups (Fig. 6a,b). The data suggests a vascular-disruptive action of drug-loaded MCLs, possibly overshadowing the advantage of using the magnet at the dose employed.

Discussion

Tumor growth is angiogenesis-dependent,[31,32] and so the suppression of tumor angiogenesis and/or the alterations in general vascular function(s) results in the suppression of local tumor growth and spread of disease. Efforts focused on destroying the tumor vascular supply are rarely influenced by physiological tumor barriers,[2] an advantage of our MDT approach.

Cationic liposomes preferentially target the tumor vasculature, and when they are loaded with chemotherapeutic agents the drug carrier molecule enhances both the delivery and antitumor effects of the drug.[4–6] The use of cationic liposome therapeutics has demonstrated promising preclinical and clinical results.[33] However, heterogeneous and non-specific targeting has created opportunities to improve on the therapeutic approach.[5,33]

The results from the present study show the successful use of the dorsal skinfold chamber to determine the extent to which magnetic fields improve tumor vascular targeting. To the best of our knowledge, the use of the small animal chamber model to assess the efficiency of MDT has never been reported elsewhere.

We also investigated whether MDT could be used to improve vinblastine therapy. Vinblastine sulfate (hydrophilic drug) is fairly effective in inhibiting the growth of melanoma and human endothelial cells (when used as a free drug or when loaded in cationic liposomes).[22] We therefore used vinblastine-loaded MCLs to evaluate our MDT strategy against (B16-F10) tumor growth. The studies showed that the antitumor activity of vinblastine when loaded in MCLs was more effective compared to vinblastine alone. This was probably owing to the enhanced delivery of the chemotherapeutic agents to the tumor vasculature, as supported by Figure 3. The use of MCLs with an external magnet further enhanced the antitumor activity of vinblastine over MCLs alone. This observation is supported by a previously published report on a study in which the percent of ^{111}In labeled MCLs recovered by the tumor was significantly greater in the presence of an external magnet.[21]

Histological evaluation of tumor sections taken from the groups exposed to vinblastine-loaded MCLs and the magnet showed a decrease in the density of neoplastic cells compared to the other treatment groups. The external magnet probably increased the therapeutic dose at the tumor site. We note also that partial embolization of tumor vessels by the magnetic particles may have contributed in part to the overall antitumor effects.[10,34,35]

The efficacy evaluation study was terminated on day 16 owing to the presence of a tough callous layer on the external surface of the tumor in some mice. This posed difficulty with the consistency of applying the magnet. Had the study continued beyond day 16, the callous layer could have altered the degree to which the magnetic field could adequately, and reproducibly, penetrate the tumor burden.

The use of an alternating magnetic field (AMF), rather than a permanent magnet, should generate a stronger and more consistent magnetic field strength. AMFs can also be fine-tuned to compensate for the callous material at the epidermal skin layer, which would otherwise terminate the studies. Another option is to employ a melanoma model capable of growing without the callous layer. B16-F10 was used for the therapeutic studies owing to the aggressive tumor phenotype, closely resembling the human pathological state, an important consideration in the design of the study. B16-F10 (melanoma) is also a highly metastatic tumor, and the presence of black pigmented tumor nodules in the liver and spleen afforded additional opportunities to both observe and distinguish differences between the treatment strategies.

We observed that the melanin pigment in the liver sections from mice treated with free drug was less compared to the saline

control group. This might be caused by the non-specific action of the vinblastine combined with the action of the active metabolites formed, since vinblastine metabolizes to active metabolites in the liver by cytochrome P450 3A[36] In general, the antitumor activity of vinblastine-loaded MCLs was superior to the effects of vinblastine alone. H&E staining of the liver and spleen sections of mice treated with the drug-loaded formulation revealed fewer tumor nodules compared to both the untreated and free drug control groups. Interestingly, whether or not the magnetic field was applied, we observed a similar decrease in the number of blood vessels for the group treated with vinblastine-loaded MCLs compared to (free drug ad untreated) controls (Fig. 6).

A functional vascular supply is required for the successful development of metastatic disease.[37,38] We observed that the use of drug-loaded MCLs in combination with an external magnet prevented (B16-F10) tumors from metastasizing to the pleural cavity. The MDT approach prevented the growth of pulmonary metastases (Fig. 5b[iv]), but the use of drug-loaded MCLs alone failed to inhibit metastatic growth to the same location (Fig. 5b[iii]). This would suggest that the magnet altered functional properties of the tumor vasculature, an unexamined area of the present study. The determination of tumor vascular density (on the final day of treatment) might not have captured differential vascular effects between the magnet and no-magnet control groups, given that vascular density is not a direct indicator of tumor vascular function.

To determine the underlying mechanism(s) involved in the MDT approach, an evaluation of tumor vascular function(s), e.g. blood flow velocity and vascular permeability measurements, in addition to structural indicators like vascular density, may improve our basic understanding of the therapeutic process. Moreover, the dose of vinblastine-loaded MCLs used was close to the maximum tolerated dose. Under these conditions we observed prominent tumor vascular defects in both the magnet and no-magnet groups. It is possible that differential vascular effects would have resulted if the dose was closer to the minimum effective concentration rather than to the maximum tolerated dose.

In summary, the magnet improved tumor vascular uptake of MCLs, enhanced the antitumor effect of drug-loaded MCLs, prevented melanoma metastasis to the pleural cavity, and compromised the tumors metastatic growth potential of melanoma to other RES organs as well. Overall, the results support the future development of MCLs for the treatment of cancer, including additional mechanistic and optimization studies.

Acknowledgments

The authors thank Chemicell for providing the fluid MAG-C used to prepare MCLs used in our study. This manuscript represents work submitted in partial fulfillment of the Doctoral Degree in Pharmaceutical Sciences, Northeastern University, Boston, MA (for S.D.). The study was funded in part by the New Investigators Scholars Program (NIP) sponsored by the American Foundation for Pharmaceutical Education (AFPE) and the Provost Research and Scholarship Grant (for R.B.C).

Disclosure Statement

None declared.

Abbreviations

B16-F10	murine melanoma
CHOL	cholesterol
DMPC	1,2-dimyristoyl-phosphatidylcholine
DMPE-PEG_{5000}	1,2-dimyristoyl-phosphatidylethanolamine-polyethylene glycol
DMTAP	1,2-dimyristoyl-trimethyl-ammonium propane
HMEC-1	human dermal microvascular endothelial cells
MAG-C	fluid MAG-CS (magnetite, citric acid matrix)
MCLs	magnetic cationic liposomes
MDT	magnetic drug targeting
MW	molecular weight
PCLs	PEGylated cationic liposomes
RES	reticuloendothetial system
TEM	transmission electron microscopy

References

1 Folkman J. Tumor Angiogenesis. *Adv Cancer Res* 1985; **43**: 175–203.
2 Chaplin DJ, Dougherty GJ. Tumour vasculature as a target for cancer therapy. *Br J Cancer* 1999; **80**(Suppl. 1): 57–64.
3 Denekamp J. Vasculature as a target for tumor therapy. *Prog Appl Microcirc* 1984; **4**: 28–38.
4 Thurston G, McLean JW, Rizen M *et al*. Cationic liposomes target angiogenic endothelial cells in tumors and chronic inflammation in mice. *J Clin Invest* 1998; **101**: 1401–13.
5 Campbell RB, Fukumura D, Brown EB *et al*. Cationic charge determines the distribution of liposomes between the vascular and extravascular compartments of tumors. *Cancer Res* 2002; **62**: 6831–6.
6 Strieth S, Eichhorn ME, Sauer B *et al*. Neovascular targeting chemotherapy: encapsulation of paclitaxel in cationic liposomes impairs functional tumor microvasculature. *Int J Cancer* 2004; **110**: 117–24.
7 Widder KJ, Senyei AE, Scarpelli DG. Magnetic microspheres: a model system for site specific drug delivery in vivo. *Proc Soc Exp Biol Med* 1978; **158**: 141–6.
8 Alexiou C, Arnold W, Klein RJ *et al*. Locoregional cancer treatment with magnetic drug targeting. *Cancer Res* 2000; **60**: 6641–8.
9 Babincova M, Altanerova V, Lampert M *et al*. Site-specific *in vivo* targeting of magnetoliposomes using externally applied magnetic field. *Z Naturforsch [C]* 2000; **55**: 278–81.
10 Kubo T, Sugita T, Shimose S, Nitta Y, Ikuta Y, Murakami T. Targeted systemic chemotherapy using magnetic liposomes with incorporated adriamycin for osteosarcoma in hamsters. *Int J Oncol* 2001; **18**: 121–5.
11 Nobuto H, Sugita T, Kubo T *et al*. Evaluation of systemic chemotherapy with magnetic liposomal doxorubicin and a dipole external electromagnet. *Int J Cancer* 2004; **109**: 627–35.
12 Zhang JQ, Zhang ZR, Yang H, Tan QY, Qin SR, Qiu XL. Lyophilized paclitaxel magnetoliposomes as a potential drug delivery system for breast carcinoma via parenteral administration: *in vitro* and *in vivo* studies. *Pharm Res* 2005; **22**: 573–83.
13 Babincova M, Cicmanec P, Altanerova V, Altaner C, Babinec P. AC-magnetic field controlled drug release from magnetoliposomes: design of a method for site-specific chemotherapy. *Bioelectrochemistry* 2002; **55**: 17–19.
14 Hassan EE, Gallo JM. Targeting anticancer drugs to the brain. I. Enhanced brain delivery of oxantrazole following administration in magnetic cationic microsperes. *J Drug Targeting* 1993; **1**: 7–14.
15 Jain TK, Morales MA, Sahoo SK, Leslie-Pelecky DL, Labhasetwar V. Iron oxide nanoparticles for sustained delivery of anticancer agents. *Mol Pharm* 2005; **2**: 194–205.
16 Fortin-Ripoche JP, Martina MS, Gazeau F *et al*. Magnetic targeting of magnetoliposomes to solid tumors with MR imaging monitoring in mice: feasibility. *Radiology* 2006; **239**: 415–24.
17 Suzuki M, Shinkai M, Honda H, Kobayashi T. Anticancer effect and immune induction by hyperthermia of malignant melanoma using magnetite cationic liposomes. *Melanoma Res* 2003; **13**: 129–35.
18 Hirao K, Sugita T, Kubo T *et al*. Targeted gene delivery to human osteocarcinoma cells with magnetic cationic liposomes under a magnetic field. *Int J Oncol* 2003; **22**: 1065–71.
19 Gang J, Park SB, Hyung W *et al*. Magnetic poly epsilon-caprolactone nanoparticles containing Fe_3O_4 and gemcitabine enhance anti-tumor effect in pancreatic cancer xenograft mouse model. *J Drug Target* 2007; **15**: 445–53.
20 Wu J, Lee A, Lu Y, Lee RJ. Vascular targeting of doxorubicin using cationic liposomes. *Int J Pharm* 2007; **337**: 329–35.
21 Dandamudi S, Campbell RB. Development and characterization of magnetic cationic liposomes for targeting tumor microvasculature. *Biochim Biophys Acta* 2007; **1768**: 427–38.

doi: 10.1111/j.1349-7006.2009.01201.x

22 Dandamudi S, Campbell RB. The drug loading, cytotoxicty and tumor vascular targeting characteristics of magnetite in magnetic drug targeting. *Biomaterials* 2007; **28**: 4673–83.
23 Maswadeh H, Demetzos C, Dimas K *et al*. Accumulation of vinblastine into transfersomes and liposomes in response to a transmembrane ammonium sulfate gradient and their cytotoxic/cytostatic activity *in vitro*. *Anticancer Res* 2001; **21**: 2577–83.
24 Ellis A. Solutions to the problem of substitution of ERL 4221 for vinyl cyclohexene dioxide in spurr low viscosity embedding formulations. *Microscopy Today* 2006: 32–3.
25 krasnici S, Werner A, Eichhorn ME *et al*. Effect of the surface charge of liposomes on their uptake by angiogenic tumor vessels. *Int J Cancer* 2003; **105**: 561–7.
26 Nair S, Boczkowski D, Moeller B, Dewhirst M, Vieweg J, Gilboa E. Synergy between tumor immunotherapy and antiangiogenic therapy. *Blood* 2003; **102**: 964–71.
27 Pluen A, Boucher Y, Ramanujan S *et al*. Role of tumor-host interactions in interstitial diffusion of macromolecules: cranial vs. subcutaneous tumors. *Proc Natl Acad Sci U S A* 2001; **98**: 4628–33.
28 Das SK, Sainsbury R. Malignant melanoma-An overview. *Indian J Dermatol* 1975; **21**: 12–20.
29 Murakami T, Cardones AR, Hwang ST. Chemokine receptors and melanoma metastasis. *J Dermatol Sci* 2004; **36**: 71–8.
30 Ishida T, Kundu RK, Yang E, Hirata K, Ho YD, Quertermous T. Targeted disruption of endothelial cell-selective adhesion molecule inhibits angiogenic processes *in vitro* and *in vivo*. *J Biol Chem* 2003; **278**: 34598–604.
31 Folkman J. What is the evidence that tumors are angiogenesis dependent? *J Natl Cancer Inst* 1990; **82**: 4–6.
32 Folkman J. The role of angiogenesis in tumor growth. *Semin Cancer Biol* 1992; **3**: 65–71.
33 Campbell RB, Ying B, Kuesters GM, Hemphill R. Fighting cancer: from the bench to bedside using second generation cationic liposomal therapeutics. *J Pharm Sci* 2009; **98**: 411–29.
34 Lubbe AS, Bergemann C, Riess H *et al*. Clinical experiences with magnetic drug targeting: a phase I study with 4′-epidoxorubicin in 14 patients with advanced solid tumors. *Cancer Res* 1996; **56**: 4686–93.
35 Barry JW, Bookstein JJ, Alksne JF. Ferromagnetic embolization. Experimental evaluation. *Radiology* 1981; **138**: 341–9.
36 Zhou-Pan XR, Seree E, Zhou XJ *et al*. Involvement Human Liver Cytochrome P450 3A in vinblastine metabolism: drug interactions. *Cancer Res* 1993; **53**: 5121–6.
37 Fidler IJ. Regulation of neoplastic angiogenesis. *J Natl Cancer Inst* 2001: 10–14.
38 Fidler IJ. Angiogenesis and cancer metastasis. *Cancer J (Sudbury, Mass* 2000; **6**(Suppl. 2): S134–41.